Talanta 225 (2021) 122074

Contents lists available at ScienceDirect

Talanta

journal homepage: www.elsevier.com/locate/talanta

Label-free photoelectrochemical biosensor for alpha-fetoprotein detection based on Au/Cs_xWO_3 heterogeneous films

Jing Li [a], Dali Liu [a,*], Donglei Zhou [a,**], Long Shao [a], Xu Chen [b], Hongwei Song [a,***]

[a] State Key Laboratory of Integrated Optoelectronics, College of Electronic Science and Engineering, Jilin University, 2699 Qianjin Street, Changchun, 130012, PR China
[b] Key Laboratory of Material Physics, Ministry of Education, School of Physics and Microelectronics, Zhengzhou University, Zhengzhou, 450000, PR China

ARTICLE INFO

Keywords:
Photoelectrochemical biosensor
Au/Cs_xWO_3 heterogeneous films
Hepatocellular carcinoma
Alpha-fetoprotein

ABSTRACT

In this work, a novel label-free photoelectrochemical (PEC) biosensor based on Au/Cs_xWO_3 heterogeneous films with low background noise and excellent sensitive detection of alpha-fetoprotein (AFP) was proposed. We prepared Au/Cs_xWO_3 heterogeneous films by different methods including template removal and spin coating. The surface plasmon resonances (SPR) of Au film and Cs_xWO_3 semiconductor nanocrystals largely improved the photoelectrochemical properties of the electrodes and enhanced the photocurrent. Under the optimal conditions, the prepared PEC biosensor showed a linear response between photocurrent variation and the logarithm of AFP concentration in the range from 0.01 ng/mL to 500 ng/mL with a low detection limit of 7 pg/mL. In addition, the proposed PEC biosensor had excellent specificity, repeatability, long-term stability and showed satisfactory results in the analysis of human serum samples, which would have great prospect in clinical application and biological analysis in the future.

1. Introduction

Hepatocellular carcinoma (HCC) is a major disease that endangers human health and life all around the world [1,2,]. The mortality rate of HCC is also relatively high in severe common cancer [3]. Early diagnosis and treatment of HCC is particularly important for the patients [4]. Meanwhile, alpha-fetoprotein (AFP) is one of the most commonly serum protein as a special tumor marker in HCC, and it is widely used in the area of screening, diagnosis, treatment, prognosis and liver transplantation of HCC [4–6]. Normally, the concentration of AFP in human serum is less than 10 ng/mL, and the exceeded concentration of AFP in adult serum is possible to lead the liver cells developing to carcinogenesis [4,6,7]. Thus, several available methods, such as electrochemical immunoassay [8,9], enzyme-linked immunoassay (ELISA) [10], fluorescence immunoassay [11–13], surface plasmon resonance (SPR) immunoassay [14], electrochemiluminescence (ECL) immunoassay [15], have been developed for detecting AFP. Despite the above methods have been achieved good sensitivity, they usually need long analysis time, high cost, complex process and so on [16]. So it is necessary for us to develop a novel, rapid and high sensitive detection method of AFP [17–19].

Photoelectrochemical (PEC) biosensors are widely regarded as a newly and powerful technique for bioanalysis, due to the better inherent sensitivity and the specific bioaffinity characteristics of the biomolecules compared with the conventional methods [19–21]. The detection principle is based on the photoelectric conversion characteristics of the photoelectric active substances to determine the concentration of the detected biomarker [17]. In the process of photoelectrochemical detection, light is used as the excitation signal to excite the photosensitive substance, while the electrical signal is used as the detection signal [18,22–24]. Therefore, the PEC analysis technique has high sensitivity [25]. Meanwhile, the PEC strategy has a great potential application prospect in the detection of small fraction and biomolecules. In the PEC biosensing, as the output signal based on the photoelectric conversion characteristics of photosensing material, the photo current is crucial to the PEC biosensor for timely detection of biomarkers [26]. Generally, according to the types of photoactive materials, they can be roughly divided into the following categories: inorganic photoactive materials, organic photoactive materials, composite photoactive materials and other materials, etc. Common inorganic photoactive materials include

* Corresponding author.
** Corresponding author.
*** Corresponding author.
E-mail addresses: ldl@jlu.edu.cn (D. Liu), zhoudl@jlu.edu.cn (D. Zhou), songhw@jlu.edu.cn (H. Song).

https://doi.org/10.1016/j.talanta.2020.122074
Received 25 September 2020; Received in revised form 26 December 2020; Accepted 26 December 2020
Available online 6 January 2021

ZnO [16,27,28], TiO_2 [29–31], CdS [25,32], WO_3 [25,32–34], reduced graphene oxide [34,35] and so on. When the photosensitive material is excited by light whose energy is larger than the band gap of photosensitive material, the ground state electrons would transfer from the valence band to conduction band, forming the electron-hole pairs and generating the photocurrent [36].

In order to enhance the photoelectric response, coupling two kinds of materials to form a heterostructure was considered as an efficient way [37,38]. The construction of heterojunction could effectively extend the photo-absorption range and inhibit the recombination of photo-generated electron-hole pairs, so that the photoelectric effect of the semiconductors can be enhanced [30,31,33,39]. Cs_xWO_3 is an inorganic semiconductor material with a narrower band gap of 2.5–2.8 eV, whose high visible light transmittance and strong absorption in the near infrared light region have attracted attention of researchers [40,41]. Moreover, Cs_xWO_3 owns the properties of excellent chemical stability, easy to synthesize, environment friendly, and good controllability of its pattern. Especially the hexagonal morphology of Cs_xWO_3 nanocrystals has strong local surface plasmon resonance (LSPR) in the near infrared absorption [41]. The Cs_xWO_3 with excellent biocompatibility and stability could be used as PEC biosensing substrate material. In addition, Au film can improve the conductivity of electrode and the efficiency of PEC biosensors because of its excellent transport performance and broaden exciton-plasmon effect in the visible region [13,42,43].

In this paper, we designed a novel label-free PEC biosensor for AFP detection based on Au/Cs_xWO_3 heterogeneous films, as shown in Scheme 1. Au/Cs_xWO_3 heterogeneous films can utilize the surface plasmon resonance of noble metal and excellent photoelectric performance of Cs_xWO_3 to enhance the photoelectric response, adjust the spectral absorption range, promote charge transfer, and significantly improve the photocurrent response. Significantly, there is still no exploration about applying Au/Cs_xWO_3 heterogeneous films in the construction of PEC biosensor up to now. Moreover, the experimental results obtained with Au/Cs_xWO_3 heterogeneous films indicate that the method is really promising for diagnosis purposes.

2. Experimental section

2.1. Materials and reagents

Methyl methacrylate (MMA), tungsten (VI) chloride (WCl_6), cesium chloride (CsCl), oleylamine (OlAm), oleic acid (OlAc) were purchased from Macklin. Sodium hydroxide (NaOH), 2-methylpropanenitrile (AIBN), potassium persulfate ($K_2S_2O_8$), ethanol, toluene, acetone, hydrogen peroxide (H_2O_2), ascorbic acid (AA) and acetic acid were bought from Beijing Chemical Works Co. Ltd. Gold chloride ($HAuCl_4$) was obtained from Aladdin. Alpha-fetoprotein (AFP), prostate specific antigen (PSA), carcinoembryonic antigen (CEA) and Anti-AFP antibody (Ab, polyclonal rabbit) were purchased from Beijing Boisynthese Biotechnology Co. Ltd. Chitosan (CS) was purchased from the solarbio Co. Ltd (China). Bovine serum albumin (BSA) was purchased from Beijing Ding Guo Biotechnology Company. The phosphate buffer solution (PBS) was prepared by conventional methods, which was at 0.01 M pH = 7.2 for perparing antigens and antibodies, at 0.1 M pH = 7.4 for cleaning and testing. Moreover, all aqueous solutions were prepared from the deionized (DI) water (18.2 MΩ·cm), which was obtained from a water purification system. All chemicals were of analytically pure specifications without further purification.

2.2. Apparatus

The UV–Visible (UV-VIS) absorption spectrum was recorded with the UV-1800PC ultraviolet–visible–near infrared (NIR) (Shimadzu, Japan). Scanning electron microscope (SEM) images were characterized by using a JEOL JSM-7500 filed emission scanning electron microscope at an accelerating voltage of 5 kV(Japan). Transmission electron microscope (TEM) image was collected on a H-800 type transmission electron microscope at an accelerating voltage of 200 kV (Japan). X-ray diffraction (XRD) patterns were carried out by a Rigaku D/max 2550 X-ray diffractometer. Electrochemical impedance spectroscopy (EIS) and electrochemical measurements were carried out on a CHI660D electrochemical workstation (Chenhua Instrument Shanghai Co. Ltd., China).

2.3. Preparation of electrode

Step A (Synthesis of PMMA nanospheres): The PMMA nanospheres were prepared according to our previous work [16]. Firstly, MMA was washed with 0.015 g/mL concentration of NaOH solution to remove the polymerization inhibitor, the above cleaning process is repeated four times over. DI water (60 mL), as-prepared MMA (6 mL) and $K_2S_2O_8$ (10 mg) were added into a 100 mL three-necked round bottom flask. The solution part of the flask was completely immersed in the oil pan, the middle neck mouth of the three-neck round bottom flask was connected with the condensation pipe, and the other two neck ports were blocked

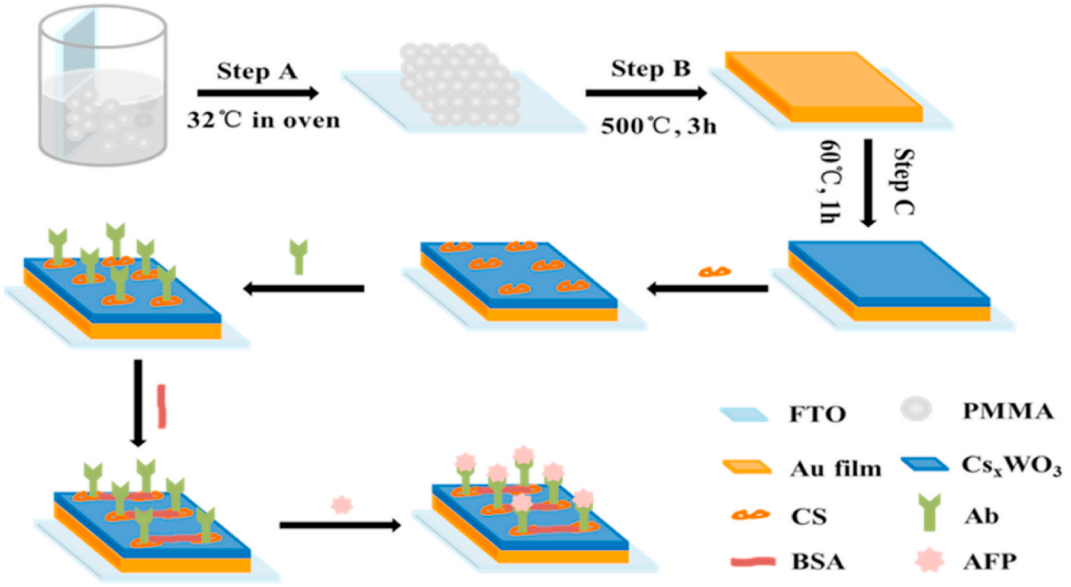

Scheme 1. Fabrication procedure of the label-free PEC biosensor.

with glass plugs. Then, the oil pan switch was turned on and the oil pan temperature was set to 90 °C under magnetic stirring of 15 rpm. By changing the amount of MMA in the above method, the diameter of PMMA ball could be primely tuned, and the expected photonic stop band (PSB) could be obtained by controlling the rate of stirring as well. Whereafter, the FTO substrate was dipped in the mixed solution of H_2O_2/H_2SO_4 (volume ratio of 1:3) for 24 h [44]. Then, the FTO substrate in turn was washed ultrasonically in DI water, the mixed solution of ethanol/acetone/sodium hydroxide (volume ratio of 1:1:1), acetone, DI water to make the surface hydrophilic. And the hydrophilic FTO substrate was immersed in the prepared PMMA colloidal suspension and placed in an oven at 32 °C for 20 h. PMMA colloidal spheres would be self-assembled into an ordered array on the FTO substrate by the surface tension produced in the process of the liquid evaporation. Finally, the PMMA templates were sintered at 120 °C for 40 min to strengthen their physical properties.

Step B (Preparation of Au film): 25 μL 1.25 M $HAuCl_4$ solution was infiltrated into the gap of the PMMA template through using capillary tension, and then dried at room temperature [43]. The dried sample was put into a 500 °C tube furnace for 3 h, and then naturally dropped to room temperature. The Au film was formed on the FTO glass, which was the FTO/Au electrode.

Step C (Preparation of Cs_xWO_3 and FTO/Au/Cs_xWO_3 electrode): Cs_xWO_3 nanocrystals were prepared according to existing colloidal synthesis method [40]. Firstly, 0.2 mmol tungsten chloride, 0.12 mmol cesium chloride, 0.6 mmol oleylamine, 19 mmol oleic acid and magnetic stirrer were added into a three-necked flask, and then magnetically stirred and heated at 300 °C for 2 h, the whole reaction above was carried out under nitrogen. Then, a dark blue solution was obtained, which was washed twice with 0.5 mL toluene and 1 mL acetone, and was centrifuged at 4000 rpm for 10 min to obtain Cs_xWO_3 nanocrystals. The synthesized Cs_xWO_3 nanocrystals were dispersed into 4 mL toluene solution, and then 40 μL of the above solution was taken to spin-coat on the surface of the FTO/Au electrode. The prepared electrode was annealed at 60 °C for 1 h, and then was rinsed with phosphate buffer (pH = 7.2) and dried at room temperature.

2.4. PEC measurements

The surface of the FTO working electrode modified with Au/Cs_xWO_3 heterogeneous film was covered with 10 μL 0.05 wt% chitosan and dried at room temperature. After thoroughly washing with NaOH solution and deionized water respectively, 20 μL 5% GLD aqueous solution was dropped onto the FTO/Au/Cs_xWO_3 electrode and maintained for 30 min at room temperature to activate chitosan. Then, the electrode was rinsed with deionized water. Subsequently, 25 μL 50 μg/mL Ab was modified on the surface of working electrode and then incubated at 4 °C for more than 12 h. After rinsing with washing buffer to remove the uncombined Ab, 20 μL 1% bovine serum albumin solution was modified to block non-specific active sites on the electrode surface for 30 min at 37 °C. After washing with PBS (pH = 7.4), 25 μL AFP antigen with different concentrations were dropped onto the prepared electrode and incubated for 1 h at 37 °C, then washed thoroughly with PBS (pH = 7.4) to get the PEC biosensor. The resulting biosensor was used in later PEC measurements.

Both the electrochemical and PEC measurement were performed using a three electrode system with a Pt wire elctrode as the counter electrode, a saturated calomel electrode (SCE) as reference electrode and the modified FTO electrode with a geometrical area of 1.0 ± 0.1 cm^2 as working electrode. All photocurrent was measured under a 500 W xenon lamp of irradiation at a constant potential of 0.6 V in 0.1 M PBS solution (pH = 7.4) containing 0.06 M AA.

3. Results and discussion

3.1. Characterizations

The TEM image of the synthesized Cs_xWO_3 nanocrystals shows that the Cs_xWO_3 nanocrystals are hexagonal prisms with an average diameter of 20 nm as shown in Fig. 1A.

The curves in Fig. 1B are the ultraviolet–visible absorption spectra of Au film, Cs_xWO_3 and Au/Cs_xWO_3 heterogeneous films. According to Fig. 2B, it can be seen that the absorption peak position of the Au film locates at about 550 nm, while the absorption peak of Cs_xWO_3 is around 830 nm. Furthermore, Au/Cs_xWO_3 heterogeneous films can realize the absorption in the visible light region and near-infrared region at the same time, and the absorption in the visible light region is enhanced relative to the Cs_xWO_3, which can improve the utilization of light and enhance the photoelectric conversion efficiency.

The X-ray diffraction (XRD) patterns of Au film, Cs_xWO_3 and Au/Cs_xWO_3 heterogeneous films are shown in Fig. 1C. According to the standard cards of Au (JCPDS 04–0784) and Cs_xWO_3 (JCPDS 81–1244), pure Au and hexagonal Cs_xWO_3 nanocrystals are obtained respectively. In addition, the diffraction peaks of Au and Cs_xWO_3 are found in the XRD pattern of the Au/Cs_xWO_3 heterogeneous films, which indicates that the Au film, Cs_xWO_3 and Au/Cs_xWO_3 heterogeneous films are successfully synthesized.

The SEM images of Au and Au/Cs_xWO_3 heterogeneous films are showed in Fig. 1D and E. It could be analyzed that the surface of the FTO/Au electrode was successfully modified with Cs_xWO_3, so that the surface of the film presents irregular compact morphology with a large surface area, which facilitates electron transfer and biomolecule immobilization. The SEM image of cross-section views of Au/Cs_xWO_3 heterogeneous films is shown in Fig. 1F.

3.2. Characterization of photoelectrochemical biosensor construction process

The stepwise process of the biosensor electrode was monitored by electrochemical impedance spectroscopy (EIS) and photocurrent responses, as illustrated in Fig. 2. EIS is normally used to analyze construction process of the biosensor electrode. The electron transfer resistance (Ret) spectra was measured in a mixture solution contains 0.1 M KCl and 0.05 M $K_3[Fe(CN)_6]/K_4[Fe(CN)_6]$ (1:1) in 0.01 M PBS (pH = 7.4) buffer solution with an open circuit voltage of 0.2 V and a frequency of 0.01 Hz–100 Hz. The electron transfer resistance (Ret) is equal to the diameter of the semicircle. As shown in Fig. 2A, Cs_xWO_3 has superconductivity, so that the electrode resistance is relatively reduced. It can be seen that the Ret of the FTO/Au/Cs_xWO_3 electrode is smaller than that of the FTO/Cs_xWO_3 electrode. The resistance increases significantly while the chitosan was modified, which is due to the insulation of chitosan [16]. Further modification of the Ab and BSA, the resistance value slightly increases, because the modification is an organic molecule, which will hinder the transfer of electrons [45]. After that, 25 μL 100 ng/mL AFP antigen was modified on the electrode surface, and the impedance spectrum also proves that the modification is successful. It proves that the label-free PEC biosensor based on Au/Cs_xWO_3 heterogeneous films is successfully prepared.

The successful preparation of PEC biosensors can also be demonstrated by the change of photocurrent. The photocurrent responses of the modified electrode for each step are shown in Fig. 2B. Fig. 2B shows that the photocurrent of the FTO/Cs_xWO_3 electrode increases relative to the bare FTO, indicating the successful modification of Cs_xWO_3, and also proving the good conductivity and photoelectric conversion performance of Cs_xWO_3. The photo current response of Au/Cs_xWO_3 heterogeneous film modified on FTO is enhanced by about 3.9 times, which proves that the heterogeneous film could significantly enhance the photoelectric conversion performance of the photoelectrochemical biosensor. This can be mainly attributed to the surface plasmonic

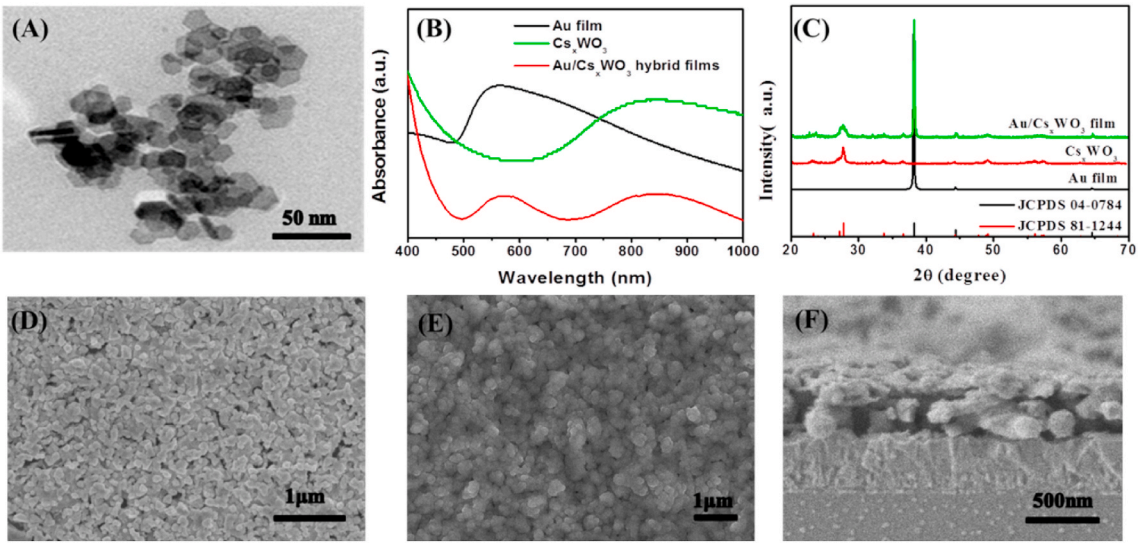

Fig. 1. (A) TEM image of Cs_xWO_3. (B) Absorption spectra of Au film, Cs_xWO_3 and Au/Cs_xWO_3 hybrid films. (C) XRD patterns of Au film, Cs_xWO_3 and Au/Cs_xWO_3 film. SEM images of Au film (D), Au/Cs_xWO_3 film (E). (F) SEM image of cross-section view of Au/Cs_xWO_3 film.

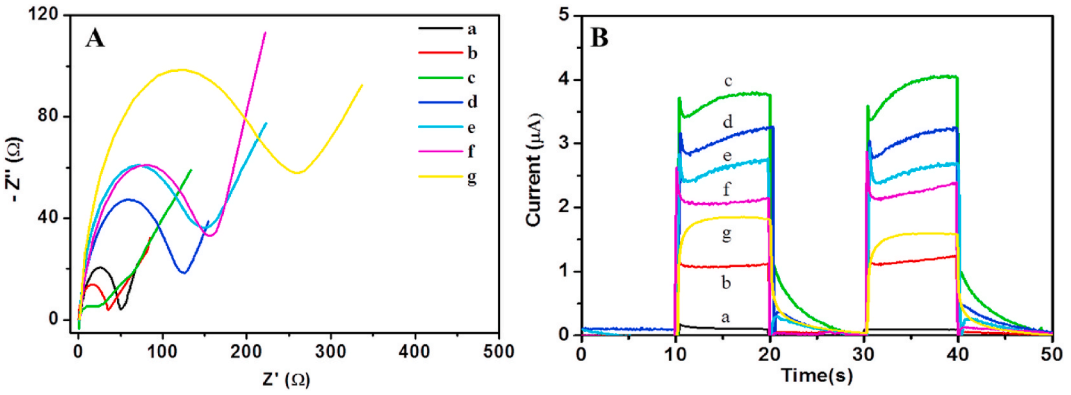

Fig. 2. Electrochemical impedance spectroscopy (EIS) (A) and Photoelectric response (B) of the modified electrode at each step: (a) FTO; (b) FTO/Cs_xWO_3; (c) FTO/Au/Cs_xWO_3; (d) FTO/Au/Cs_xWO_3/CS; (e) FTO/Au/Cs_xWO_3/CS/Ab; (f) FTO/Au/Cs_xWO_3/CS/Ab/BSA; (g) FTO/AuCs_xWO_3/CS/Ab/BSA/AFP.

resonance of noble metal and the excellent photoelectric performance of Cs_xWO_3, which can enhance the photoelectric response, promote charge transfer, and significantly improve the photocurrent [41,42]. Then, when the surface of the electrode was modified with CS, Ab, BSA, and AFP antigen, it can be seen that the current decreases sequentially, because these substances are belong to organic molecules, which hinders the transmission of electrons and reduced the current response [46]. By detecting the change of photocurrent, it proves that the label-free PEC biosensor based on Au/Cs_xWO_3 heterogeneous film was successfully prepared.

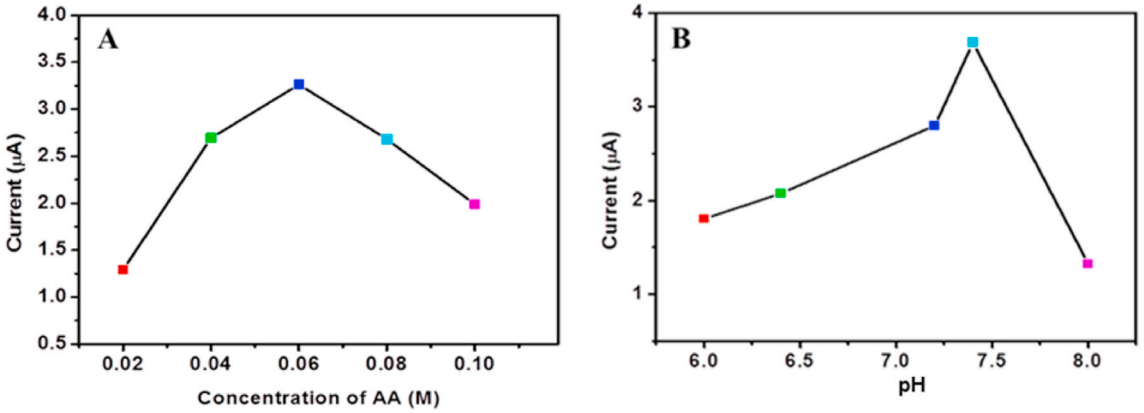

Fig. 3. (A) Current responses at different concentrations of AA. (B) Current responses at different pH values (6.0–8.0) of detection solutions.

3.3. Optimization of the detection conditions

In order to prepare a satisfactory PEC biosensor, the experimental parameters of AA concentration and pH value were optimized. Ascorbic acid (AA) served as an electron donor in the detection solution, and at the same time it could inhibit the electron-hole recombination to a certain extent to obtain a stable and sufficient photocurrent signal [47]. Therefore, the concentration of AA as a key parameter was studied in Fig. 3A. The photocurrent intensity increases as the AA concentration increased from 0.02 M to 0.06 M, and decreases when the AA concentration increases from 0.06 M to 0.1 M. This phenomenon indicates that 0.06 M AA is sufficient to form saturated electron donors for providing enough electrons in the photoinduced holes. The results shows that 0.06 M AA is the optimal concentration determined by PEC biosensor. Further, pH value could affect the activity of the biomolecules modified on the electrode, so that the photoelectric response of the electrode would be affected [48]. It can be seen from Fig. 3B, the highest photocurrent value is obtained when pH = 7.4, so this value is selected as the best pH for detection.

3.4. Photoelectrochemical detection of AFP

Under the optimum conditions, the different concentrations of AFP (25 μL) were detected by tracking the photocurrent variation of the designed PEC biosensor. Fig. 4A shows the calibration curve of the photocurrent response of different concentrations of AFP. It can be seen that the photocurrent decrement is proportional to the logarithmic value of AFP concentration, ranging from 0.01 ng/mL to 500 ng/mL. The regression equation is $\Delta I = 3.43 - 0.35 \log C_{AFP}$, with a determination coefficient of 0.997. The ΔI is the photocurrent of Au/Cs_xWO_3/CS/Ab/BSA/heterogeneous film electrode incubated with 25 μL different concentrations of AFP [48]. As the concentration of AFP increases, more and more AFP partly consumes the AA electron donor and blocks the electron transfer, resulting in gradually reduced photocurrent intensity. The PEC biosensor shows better detection limit of 7 pg/mL, which is calculated according to the previous report [46]. This as-prepared PEC biosensor shows wider linear range and lower detection limit compared with the performance of heterostructure photoelectrochemical biosensors based on other materials for AFP detection. (Table S1, Supporting information), which demonstrates that the performance of the PEC biosensor based on Au/Cs_xWO_3 heterogeneous film is acceptable and promising.

In addition, the relative standard deviation (RSD) was tested by adding different concentrations of AFP standard solutions into the human standard serum. As can be seen from Table S2, the RSD values are less than 6%, and the analysis recovery ranges are 97–104%. This shows that the label-free PEC biosensor based on Au/Cs_xWO_3 heterogeneous film has high sensitivity and accuracy for detecting AFP in real samples.

3.5. Specificity, reproducibility, stability of the PEC biosensor

In order to evaluate the specificity of the proposed biosensor for AFP, several interfering species, such as PSA, CEA and AA were added. As illustrated in Fig. 4B, the photocurrent responses originated from specific binding were obtained from four electrodes prepared with 10 ng/mL AFP and 100 ng/mL interfering proteins. There is no obvious changes in photocurrent, indicating that the photocurrent is not influenced by non-specific adsorption, so the label-free PEC biosensor based on Au/Cs_xWO_3 heterogeneous film has excellent specificity.

We kept the same experimental conditions to prepare the six PEC biosensors to test the photoelectric response of the AFP concentration of 10 ng/mL. As shown in Fig. 4C, the photocurrent of the six PEC biosensors does not change significantly, indicating that the label-free PEC biosensor based on Au/Cs_xWO_3 heterogeneous film has good repeatability.

Fig. 4D shows the long-term stability of Au/Cs_xWO_3 heterogeneous film electrode, which was storaged in a refrigerator at 4 °C. 10 ng/mL AFP was measured every 5 days, as can be seen from Fig. 4D, the photocurrent gradually decreases with the increase of time, and the electrode can still maintain 91.56% performance after 20 days,

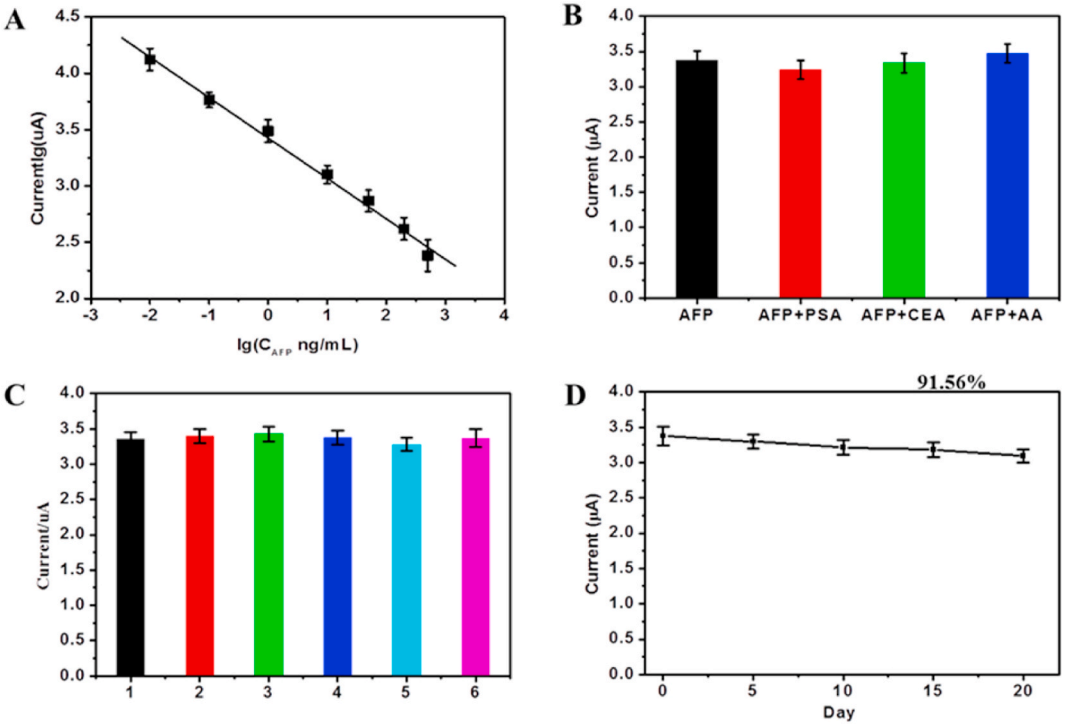

Fig. 4. (A) Calibration curve of Au/Cs_xWO_3 heterogeneous film electrode for different concentrations of AFP. (B) Specificity of the biosensors with 10 ng/mL of AFP without or with 100 ng/mL of PSA, 100 ng/mL of CEA and 100 ng/mL of AA respectively. (C) Reproducibility of the immunoassay by detecting 10 ng/mL AFP samples with six electrodes. (D) Long-term stability of the biosensor.

indicating that the label-free PEC biosensor based on Au/Cs_xWO_3 heterogeneous film had satisfactory long-term stability.

4. Conclusions

In summary, we successfully designed a novel label-free PEC biosensor based on Au/Cs_xWO_3 heterogeneous films for AFP detection. Au/Cs_xWO_3 heterogeneous films could utilize the surface plasmon resonance of the noble metal and excellent photoelectric performance of Cs_xWO_3 to enhance the photoelectric response, adjust the spectral absorption range, promote charge transfer, and significantly improve the photocurrent. This was also the first time that the Au/Cs_xWO_3 heterogeneous films had been applied to photoelectrochemical bioassay. In the best detection conditions, the detection linear range was 0.01 ng/mL to 500 ng/mL and the detection limit was 7 pg/mL. Besides, the as-prepared PEC biosensor had good specificity, repeatability, long-term stability and showed satisfactory results in the analysis of human serum samples. Therefore, the label-free photoelectrochemical biosensor based on Au/Cs_xWO_3 heterogeneous films could be applied to detect cancer markers in clinical and biological analysis in the future.

Credit author statement

Jing Li, Investigation, Writing – original draft, Software. Dali Liu, Funding acquisition, Supervision, Writing – review & editing. Donglei Zhou, Writing – review & editing, Visualization, Supervision. Long Shao, Data curation. Xu Chen, Resources. Hongwei Song, Funding acquisition, Supervision, Project administration.

Declaration of competing interest

The authors declare that they have no known competing financial interests or personal relationships that could have appeared to influence the work reported in this paper.

Acknowledgements

This work was supported by the Key Program of NSFC-Guangdong Joint Funds of China (U1801253), National Key Research and Development Program (2016YFC0207101), the National Natural Science Foundation of China (Grant Nos. 61974175, 61822506, 11874181, 61874049, 61775080, 11674126, 11674127, 61674067, 11904124), the Special Project of the Province-University Co-constructing Program of Jilin Province (SXGJXX2017-3), the Jilin Province Natural Science Foundation of China (No. 20180101210JC, 20170101170JC).

Appendix A. Supplementary data

Supplementary data to this article can be found online at https://doi.org/10.1016/j.talanta.2020.122074.

References

[1] R.L. Siegel, K.D. Miller, A. Jemal, Cancer statistics, CA A Cancer J. Clin. 69 (2019) 7–34, 2019.
[2] M.A. Avila, C. Berasain, B. Sangro, J. Prieto, New therapies for hepatocellular carcinoma, Oncogene 25 (2006) 3866–3884.
[3] H.S. Kim, J.D. Yang, H.B. El-Serag, F. Kanwal, Awareness of chronic viral hepatitis in the United States: an update from the national health and nutrition examination survey, J. Viral Hepat. 26 (2019) 596–602.
[4] E.N. Debruyne, J.R. Delanghe, Diagnosing and monitoring hepatocellular carcinoma with alpha-fetoprotein: new aspects and applications, Clinica chimica acta, international journal of clinical chemistry 395 (2008) 19–26.
[5] A. Riaz, R.K. Ryu, L.M. Kulik, M.F. Mulcahy, R.J. Lewandowski, J. Minocha, et al., Alpha-fetoprotein response after locoregional therapy for hepatocellular carcinoma: oncologic marker of radiologic response, progression, and survival, J. Clin. Oncol. : official journal of the American Society of Clinical Oncology 27 (2009) 5734–5742.
[6] D. Li, T. Mallory, S. Satomura, AFP-L3_ a new generation of tumor marker for hepatocellular carcinom, Clin. Chim. Acta 313 (2001) 15–19.
[7] X. Zhang, J. Sun, J. Liu, H. Xu, B. Dong, X. Sun, et al., Label-free electrochemical immunosensor based on conductive Ag contained EMT-style nano-zeolites and the application for α-fetoprotein detection, Sensor. Actuator. B Chem. 255 (2018) 2919–2926.
[8] N. Ma, T. Zhang, D. Fan, X. Kuang, A. Ali, D. Wu, et al., Triple amplified ultrasensitive electrochemical immunosensor for alpha fetoprotein detection based on MoS2@Cu2O-Au nanoparticles, Sensor. Actuator. B Chem. 297 (2019) 126821.
[9] D. Sun, H. Li, M. Li, C. Li, L. Qian, B. Yang, Electrochemical immunosensors with AuPt-vertical graphene/glassy carbon electrode for alpha-fetoprotein detection based on label-free and sandwich-type strategies, Biosens. Bioelectron. 132 (2019) 68–75.
[10] S.K. Arya, P. Estrela, Recent advances in enhancement strategies for electrochemical ELISA-based immunoassays for cancer biomarker detection, Sensors 18 (2018).
[11] L. Zhou, F. Ji, T. Zhang, F. Wang, Y. Li, Z. Yu, et al., An fluorescent aptasensor for sensitive detection of tumor marker based on the FRET of a sandwich structured QDs-AFP-AuNPs, Talanta 197 (2019) 444–450.
[12] Y. Zhou, X. Huang, S. Xiong, X. Li, S. Zhan, L. Zeng, et al., Dual-mode fluorescent and colorimetric immunoassay for the ultrasensitive detection of alpha-fetoprotein in serum samples, Anal. Chim. Acta 1038 (2018) 112–119.
[13] S. Xu, B. Dong, D. Zhou, Z. Yin, S. Cui, W. Xu, et al., Paper-based upconversion fluorescence resonance energy transfer biosensor for sensitive detection of multiple cancer biomarkers, Sci. Rep. 6 (2016) 23406.
[14] H. Wang, X. Wang, J. Wang, W. Fu, C. Yao, A SPR biosensor based on signal amplification using antibody-QD conjugates for quantitative determination of multiple tumor markers, Sci. Rep. 6 (2016) 33140.
[15] D. Pan, K. Chen, Q. Zhou, J. Zhao, H. Xue, Y. Zhang, et al., Engineering of CdTe/SiO2 nanocomposites: enhanced signal amplification and biocompatibility for electrochemiluminescent immunoassay of alpha-fetoprotein, Biosens. Bioelectron. 131 (2019) 178–184.
[16] R. Xu, Y. Jiang, L. Xia, T. Zhang, L. Xu, S. Zhang, et al., A sensitive photoelectrochemical biosensor for AFP detection based on ZnO inverse opal electrodes with signal amplification of CdS-QDs, Biosens. Bioelectron. 74 (2015) 411–417.
[17] W.-W. Zhao, M. Xiong, X.-R. Li, J.-J. Xu, H.-Y. Chen, Photoelectrochemical bioanalysis: a mini review, Electrochem. Commun. 38 (2014) 40–43.
[18] W.W. Zhao, J.J. Xu, H.Y. Chen, Photoelectrochemical Bioanalysis: the State of the Art, Chemical Society reviews2015, pp. 729-741.
[19] A. Devadoss, P. Sudhagar, C. Terashima, K. Nakata, A. Fujishima, Photoelectrochemical biosensors: new insights into promising photoelectrodes and signal amplification strategies, J. Photochem. Photobiol. C Photochem. Rev. 24 (2015) 43–63.
[20] Y.-C. Zhu, L. Zhang, N. Zhang, W.-W. Zhao, Y.-Y. Liang, J.-J. Xu, et al., Photoelectrochemical bioanalysis of protein biomarkers, Current Opinion in Electrochemistry 10 (2018) 120–125.
[21] W.W. Zhao, J.J. Xu, H.Y. Chen, Photoelectrochemical immunoassays, Anal. Chem. 90 (2018) 615–627.
[22] W.W. Zhao, J.J. Xu, H.Y. Chen, Photoelectrochemical DNA biosensors, Chem. Rev. 114 (2014) 7421–7441.
[23] W.-W. Zhao, J.-J. Xu, H.-Y. Chen, Photoelectrochemical enzymatic biosensors, Biosens. Bioelectron. 92 (2017) 294–304.
[24] F. Bettazzi, I. Palchetti, Photoelectrochemical genosensors for the determination of nucleic acid cancer biomarkers, Current Opinion in Electrochemistry 12 (2018) 51–59.
[25] R. Wang, H. Ma, Y. Zhang, Q. Wang, Z. Yang, B. Du, et al., Photoelectrochemical sensitive detection of insulin based on CdS/polydopamine co-sensitized WO3 nanorod and signal amplification of carbon nanotubes@polydopamine, Biosens. Bioelectron. 96 (2017) 345–350.
[26] X. Zhang, Y. Guo, M. Liu, S. Zhang, Photoelectrochemically active species and photoelectrochemical biosensors, RSC Adv. 3 (2013) 2846–2857.
[27] R. Yang, X. Yan, Y. Li, X. Zhang, J. Chen, Nitrogen-doped porous carbon-ZnO nanopolyhedra derived from ZIF-8: new materials for photoelectrochemical biosensors, ACS Appl. Mater. Interfaces 9 (2017) 42482–42491.
[28] Y. Jiang, D. Liu, Y. Yang, R. Xu, T. Zhang, K. Sheng, et al., Photoelectrochemical detection of alpha-fetoprotein based on ZnO inverse opals structure electrodes modified by Ag2S nanoparticles, Sci. Rep. 6 (2016) 38400.
[29] X. Pang, J. Pan, L. Wang, W. Ren, P. Gao, Q. Wei, et al., CdSe quantum dot-functionalized TiO2 nanohybrids as a visible light induced photoelectrochemical platform for the detection of proprotein convertase subtilisin/kexin type 6, Biosens. Bioelectron. 71 (2015) 88–97.
[30] P. Gao, H. Ma, T. Yan, D. Wu, X. Ren, J. Yang, et al., Construction of dentate bonded TiO2-CdSe heterostructures with enhanced photoelectrochemical properties: versatile labels toward photoelectrochemical and electrochemical sensing, Dalton Trans. 44 (2015) 773–781.
[31] X. Chen, J. Li, G. Pan, W. Xu, J. Zhu, D. Zhou, et al., Ti3C2 MXene quantum dots/TiO2 inverse opal heterojunction electrode platform for superior photoelectrochemical biosensing, Sensor. Actuator. B Chem. 289 (2019) 131–137.
[32] Q. Han, R. Wang, B. Xing, T. Zhang, M.S. Khan, D. Wu, et al., Label-free photoelectrochemical immunoassay for CEA detection based on CdS sensitized WO3@BiOI heterostructure nanocomposite, Biosens. Bioelectron. 99 (2018) 493–499.
[33] J. Su, L. Guo, N. Bao, C.A. Grimes, Nanostructured WO(3)/BiVO(4) heterojunction films for efficient photoelectrochemical water splitting, Nano Lett. 11 (2011) 1928–1933.

[34] B. Sun, K. Zhang, L. Chen, L. Guo, S. Ai, A novel photoelectrochemical sensor based on PPIX-functionalized WO3-rGO nanohybrid-decorated ITO electrode for detecting cysteine, Biosens. Bioelectron. 44 (2013) 48–51.
[35] Y. Wang, Y. Wang, D. Wu, H. Ma, Y. Zhang, D. Fan, et al., Label-free electrochemical immunosensor based on flower-like Ag/MoS 2/rGO nanocomposites for ultrasensitive detection of carcinoembryonic antigen, Sensor. Actuator. B Chem. 255 (2018) 125–132.
[36] Y. Zang, J. Fan, Y. Ju, H. Xue, H. Pang, Current Advances in Semiconductor Nanomaterial-Based Photoelectrochemical Biosensing, Chemistry 24 (2018) 14010–14027.
[37] B. Wang, J.T. Cao, Y.M. Liu, Recent progress of heterostructure-based photoelectrodes in photoelectrochemical biosensing: a mini review, Analyst 145 (2020) 1121–1128.
[38] Y.X. Dong, J.T. Cao, B. Wang, S.H. Ma, Y.M. Liu, Spatial-resolved photoelectrochemical biosensing array based on a CdS@g-C3N4 heterojunction: a universal immunosensing platform for accurate detection, ACS Appl. Mater. Interfaces 10 (2018) 3723–3731.
[39] Y. Liu, H. Zeng, Y. Chai, R. Yuan, H. Liu, Ti3C2/BiVO4 Schottky junction as a signal indicator for ultrasensitive photoelectrochemical detection of VEGF165, Chem. Commun. 55 (2019) 13729–13732.
[40] T.M. Mattox, A. Bergerud, A. Agrawal, D.J. Milliron, Influence of shape on the surface plasmon resonance of tungsten bronze nanocrystals, Chem. Mater. 26 (2014) 1779–1784.
[41] Y. Ji, W. Xu, D. Li, D. Zhou, X. Chen, N. Ding, et al., Semiconductor plasmon enhanced monolayer upconversion nanoparticles for high performance narrowband near-infrared photodetection, Nanomater. Energy 61 (2019) 211–220.
[42] J. Kim, U.G. Hong, Y. Choi, S. Hong, Enhancing the evanescent field in TiO2/Au hybrid thin films creates a highly sensitive room-temperature formaldehyde gas biosensor, Colloids Surf. B Biointerfaces 182 (2019) 110303.
[43] X. Chen, W. Xu, L. Zhang, X. Bai, S. Cui, D. Zhou, et al., Large upconversion enhancement in the “islands” Au-Ag alloy/NaYF4: Yb3+, Tm3+/Er3+Composite films, and fingerprint identification, Adv. Funct. Mater. 25 (2015) 5462–5471.
[44] L. Zhang, B. Dong, L. Xu, X. Zhang, J. Chen, X. Sun, et al., Three-dimensional ordered ZnO–Fe3O4 inverse opal gas sensor toward trace concentration acetone detection, Sensor. Actuator. B Chem. 252 (2017) 367–374.
[45] X. Wang, R. Xu, X. Sun, Y. Wang, X. Ren, B. Du, et al., Using reduced graphene oxide-Ca:CdSe nanocomposite to enhance photoelectrochemical activity of gold nanoparticles functionalized tungsten oxide for highly sensitive prostate specific antigen detection, Biosens. Bioelectron. 96 (2017) 239–245.
[46] D. Huang, L. Wang, Y. Zhan, L. Zou, B. Ye, Photoelectrochemical biosensor for CEA detection based on SnS2-GR with multiple quenching effects of Au@CuS-GR, Biosens. Bioelectron. 140 (2019) 111358.
[47] J. Li, X. Lin, Z. Zhang, W. Tu, Z. Dai, Red light-driven photoelectrochemical biosensing for ultrasensitive and scatheless assay of tumor cells based on hypotoxic AgInS2 nanoparticles, Biosens. Bioelectron. 126 (2019) 332–338.
[48] Y. Zhai, D. Liu, Y. Jiang, X. Chen, L. Shao, J. Li, et al., Near-infrared-light-triggered photoelectrochemical biosensor for detection of alpha-fetoprotein based on upconversion nanophosphors, Sensor. Actuator. B Chem. 286 (2019) 468–475.